Desalination and Water Treatment
www.deswater.com

doi:10.5004/dwt.2018.22925

124 (2018) 326–335
August

A high efficiency and rapid adsorbent for removing sunset yellow FCF by amine-modified microporous polymer

Jingshuang Fan, Yunxiafei Ling, Chao Gao, Haixia Lyu*

College of Materials Science and Engineering, Fuzhou University, Fuzhou, 350108, China, Tel. 17805931865, email: 1127706985@qq.com (J. Fan), Tel. 17805931865, email: Ling_YXF@163.com(Y. Ling), Tel. 17805931865, email: 963700776@qq.com (C. Gao), Tel. 8659122866131, email: hx_lv@163.com(H. Lyu)

Received 16 December 2017; Accepted 8 August 2018

ABSTRACT

A high specific surface area amine-modified polymer of intrinsic microporosity (NH_2-PIM-1) was synthesized by reducing nitriles to amines in the polymer of intrinsic microporosity (PIM-1) as an adsorbent to remove sunset yellow FCF (SY) from aqueous solution. The physicochemical properties of NH_2-PIM-1 were characterized by infrared spectra (IR), scanning electron microscope (SEM), thermogravimetric analysis (TGA), nuclear magnetic resonance (NMR) and N_2 adsorption-desorption isotherms measurement. The effect of initial solution pH value, dosage of adsorbent, contact time and initial SY concentration were systematically investigated. The sunset yellow FCF adsorption equilibrium was attained after 10 min and the adsorption capacity could reach 348.16 mg/g, which was superior to most of the other adsorbents previously reported. Kinetics and isothermal model experiments indicated that the adsorption of sunset yellow matched the pseudo-second-order kinetic model and Langmuir model, respectively. Thermodynamic analysis showed that the adsorption was endothermic, spontaneous and physical adsorption process. These results suggested that the NH_2-PIM-1 was a rapid and efficient kind of adsorbent for removal of sunset yellow FCF.

Keywords: Amine modified PIM-1; Sunset yellow FCF; Rapid adsorption

1. Introduction

Dye effluents discharged from dye industries, including textile, printing, food, etc., have become one of the major pollution sources of water [1]. Excessive colorful dyes and their derivatives in the water are difficultly degradable, highly toxic, mutagenic and teratogenic effects on aquatic life, which constantly threaten ecological equilibrium and human health [2,3]. Thus, it becomes necessary to remove these dyes before they are mixed with natural and unpolluted water bodies [4].

So far, various methods of treating dye wastewater are reported, such as focculation [5], oxidation [6], coagulation [7], enzymatic catalysis [8], photocatalytic degradation [9], biodegradation [10], membrane separation [11], ion exchange [12,13] and adsorption [14]. Among these technologies, adsorption is the most common due to high efficiency, low cost, non-toxicity and simplicity. The preparation of adsorbent was critical for adsorption. Therefore, the development of new modified adsorbing material and its application are receiving more and more attention. Nowadays, agricultural solid wastes [15], chitosan [16], silica gels [17] and activated carbons [18,19] have been tested to remove dyes from aqueous solution. Wu [16] synthesized Fe_3O_4/ZrO_2-CMCS nanocomposite, and the adsorption capacity of SY over this nanocomposite was 143.2 mg/g. Liu [17] synthesized polyaspartate-modified silica gels (SG-pA) as an adsorbent for methylene blue (MB) removal with a maximum adsorption capacity of 90.2 mg/g, and the adsorption reached to equilibrium in 540 min. However, these adsorbents were deficient in adsorption capacities or efficiencies. The preparation of the efficient, fast, stable, low-cost and environment-friendly absorption materials is still research main task. Goscianska [19] synthesized ordered mesoporous

*Corresponding author.

carbons modified with cerium as a high surface area adsorbent (908–987 $m^2 \cdot g^{-1}$) for sunset yellow (SY) removal with a maximum adsorption capacity of 323.91 mg/g. Therefore, the large surface area and many adsorption sites materials may provide a new way to solve this problem [20–23].

Polymer of intrinsic microporosity (PIM) is a new class of porous polymer that possesses high free volume, high specific surface area and a high affinity for organic species [24], which make it successfully applied in membrane gas separation, organics adsorption [25,26], heterogeneous catalysis and hydrogen storage [27]. Satilmis [28] modified PIM-1 with ethanolamine and diethanolamine to enhance CO_2/N_2 selectivity,and the dye adsorption study showed a good selectivity for anionic dye for 72 h of adsorption time. Zhang [28] prepared electrospun PIM-1 fibers to remove 95% oil red o and solvent blue 35 from methanol in less than 20 min. As its structure advantages of pore structure and available chemical modification, PIMs can be also used as a promising adsorbent for dye removal. In the adsorption process, the groups of $-NH_2$ on the surface of the adsorbents can be protonated by the proton reaction and the groups of $-NH_3^+$ with cationic charges can absorb the anionic pollutants through electrostatic adsorption [29–32]. Thus an efficient adsorbent can be obtained by utilizing amine-modified PIM-1. However, to the best of our knowledge, there are a few reports on utilizing amine-modified PIM-1 (NH_2-PIM-1), as an effective adsorbent for fast removing sunset yellow FCF food dye (SY) with high capacity.

In this study, we synthesized NH_2-PIM-1 via reducing nitriles to primary amines by borane tetrahydrofuran complex and used as adsorbents to remove anionic dye sunset yellow FCF (SY) (Fig. 1). The physicochemical properties of NH_2-PIM-1 were characterized by different instruments such as SEM, BET, TGA and FTIR. The effects of the parameters during the removal process including pH, dosage of adsorbent, contact time and initial SY concentration were systematically investigated in batch experiments to optimize the adsorption conditions. The kinetics, isotherms and thermodynamics of sunset yellow FCF adsorption onto NH_2-PIM-1 have also been discussed. The experimental results showed that NH_2-PIM-1 could remove SY from aqueous solution efficiently. This study can provide a reference to treat dyes wastewater by using inexpensive, efficient and easily-obtained the modified composites.

2. Materials and methods

2.1. Reagents and apparatus

5,5´,6,6´-Tetrahydroxy-3,3,3´,3´-tetramethyl-1,1´-spirobisindane (TTSBI, 96.0%) was purchased from Tokyo Chemical Industry (Shanghai, China). Tetrafluoroterephthalonitrile (TFTPN, 99%), sunset yellow FCF (SY, 87%) and borane-tetrahydrofuran (1.0 mol/L in THF, with <0.005 mol/L sodium borohydride stabilizer) were purchased from Aladdin Chemistry Co., Ltd. Anhydrous potassium carbonate, dimethylformamide (DMF), methanol, tetrahydrofuran (THF), dioxane and acetone with the analytical reagent grade were brought from Sinopharm Chemical Reagent Company (Shanghai, China).

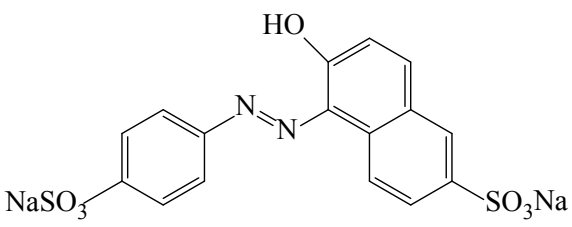

Fig. 1. Structure of sunset yellow FCF.

All pH value adjustments were measured with a digital pHS-10C pH meter (Xiaoshan Instrument Factory, Hangzhou, China). The FT-IR spectra was measured on a Nicolet 5700-Fourier transform infrared spectrometer (Thermo Electron Scientific Instruments Corp. America) at room temperature. Scanning electron microscope (SEM) pictures was measured on ZEISS SUPRA 55 (Germany). The specific surface area was measured at 77K by nitrogen adsorption-desorption isotherms with a surface area analyzer (ASAP 2020, Micromeritics Instrument Corp., America), which was calculated with the Brunauer–Emmett–Teller (BET) method. NMR spectra were measured using a Bruker Avance III 400 MHz instrument using an adamantane reference.

2.2. Preparations

2.2.1. Preparation of PIM-1

PIM-1 was synthesized at 65°C according to the procedure described by Bekir Satilmis [25]. Briefly, TTSBI (5.1062 g, 15 mmol) and TFTPN (3.0013 g, 15 mmol) were stirred and dissolved in 100 mL DMF at 65°C under nitrogen. Then, anhydrous potassium carbonate (5.1248 g, 37.08 mmol) was added to the system and the reaction mixture was stirred for 72 h. When the reaction finished, the mixture was cooled down then poured into 150 mL H_2O. The crude yellow product was collected by filtration. The filter cake was stirred in 350 mL H_2O for 15 min, recollected by filtration under vacuum and dried in an oven at 110°C for 12 h. Subsequently, the product was successively washed and filtered by 300 mL dioxane, 100 mL acetone, 200 mL H_2O and a further portion of 100 mL acetone. The final product was obtained after dried at 110°C for 12 h.

2.2.2. Amine modification of PIM-1

The primary amines on NH_2-PIM-1 were obtained by reducing nitriles on PIM-1 with borane tetrahydrofuran complex [33]. Specifically, PIM-1 solid (2 g) was added in THF (130 mL) with magnetic stirring in a nitrogen atmosphere at room temperature. Then the system was cooled down to 0°C for 15 min. With continuous stirring, borane-tetrahydrofuran (1.0 mol/L, 25 mL) was added by dropwise into the reaction mixture. And the mixtures react In the reflux device for 12 h with the help of magnetic stirring. Then the system was cooled to room temperature. To get rid of the excess borane, ethanol (80 mL) was added to the system drop by drop. The crude product was filtered under vacuum and then stirred in methanolic HCl solution (1.0 mol/L, 120 mL) for 12 h. Subsequently, the filter cake was washed to neutral. Similarly, the solid was washed again by 5% NaOH solution (200 mL) for 3 h. And the solid

was rinsed with water to adjust value of pH to neutral. The final product was obtained after dried at 110°C for 12 h.

The synthetic process is shown in Fig. 2.

2.3. Adsorption experiments

Batch experiments were performed to investigate the effects of important parameters such as initial solution pH value, dosage of adsorbent, contact time and initial SY concentration on removal of SY dye by NH_2-PIM-1. In order to optimize these parameters, 10 mL of SY solution (100 mg/L) and 5 mg adsorbent were added into a 50 mL centrifuge tube, and then the pH was adjusted to the desired value with 0.1 mol/L HCl. The adsorption process was in the assist of a magnetic stirrer and a centrifuge for an appropriate period of time. The SY solution was withdrawn for analysis by using an UV-Vis spectrophotometer (UV-2450, Shimadzu) at 482 nm. The extraction percentage (E, %) and the adsorption capacity (Q, mg/g) at equilibrium and each time segment were calculated by the following equations [32], respectively:

$$E = 100(C_0 - C_e) / C_0 \quad (1)$$

$$Q = (C_0 - C_e)V / m \quad (2)$$

where C_0 and C_e are the initial and equilibrium dye concentrations in solution, respectively (mg·L^{-1}), m is the mass (g) of the adsorbent and V is the volume of the solution (L).

3. Results and discussion

3.1. Characterization of NH_2-PIM-1

3.1.1. FTIR and ^{13}C NMR

The process of converting nitrile into amino groups can be confirmed by IR. As shown in Fig. 3, the bands at 2241 cm^{-1} and 1263 cm^{-1} were attributed to the characteristic nitrile and ether stretches in the spectrum of PIM-1. In addition, aliphatic and aromatic C-H stretches can be seen in the region 2800–3010 cm^{-1} which were consistent with the literature [25]. But in the spectrum of NH_2-PIM-1 products, the new bands' appearence of N-H stretch vibration (3382 cm^{-1}) and N-H bending vibration (813 cm^{-1}) revealed that the nitrile groups were reduced into amino groups respectively, complying with the literature [33]. Solid-state 13C NMR spectra of PIM-1 and NH_2-PIM-1 were shown in Fig. 4. Compared with peaks of PIM-1, the aromatic peak (94 ppm)labeled 11 shifted to the peak (118 ppm) of NH_2-PIM-1. And the peak labeled 12 was merged in $-CH_3$, which was consistent with the literature [25]. Therefore, it can be reasonably concluded that polymer of intrinsic microporosity (PIM-1) have been successfully modified with amine.

3.1.2. SEM and BET

Scanning electron microscopy (SEM) images of the morphology of PIM-1 (a–c) and NH_2-PIM-1 (d) were depicted in Fig. 5, respectively. It was shown that PIM-1 (a) was rough heterogeneous agglomerate microspheres with each spherical diameter of a couple hundred micrometers. And the broken parts of spheres (b-c) revealed an irregular interconnected porous network structures inside the particles. After amino modification, as shown in Fig. 5d, the spherical morphology was destroyed and the cellular frame was col-

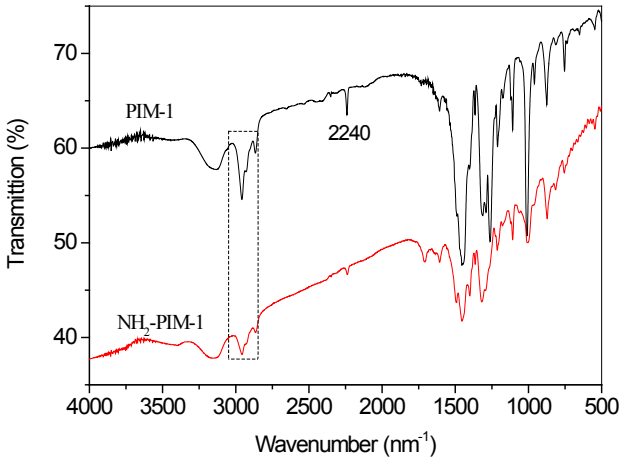

Fig. 3. FTIR spectra of PIM-1and NH_2-PIM-1.

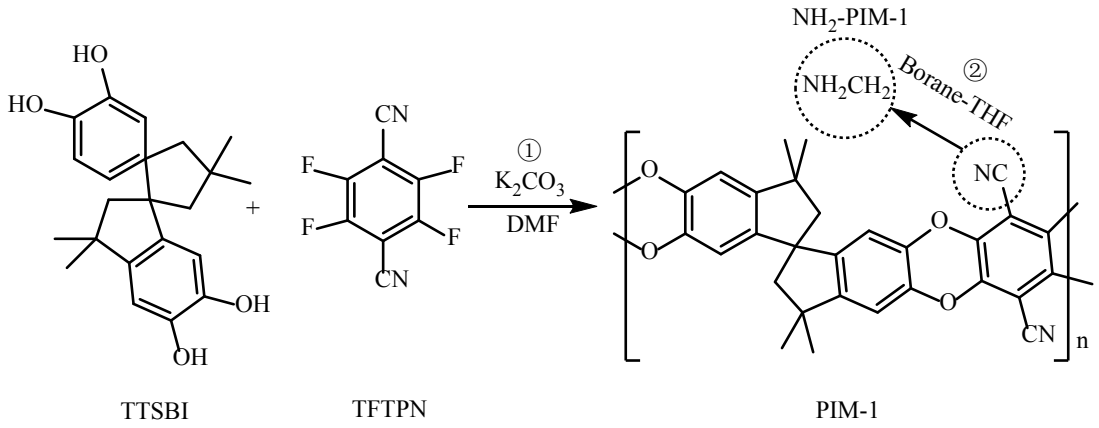

Fig. 2. Synthetic process of NH_2-PIM-1.

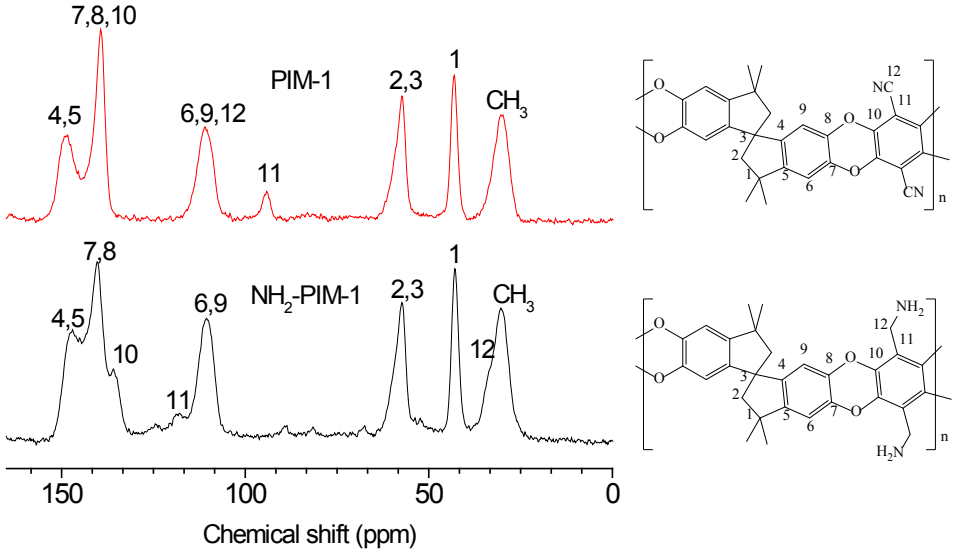

Fig. 4. ^{13}C NMR spectra of PIM-1 and NH_2-PIM-1.

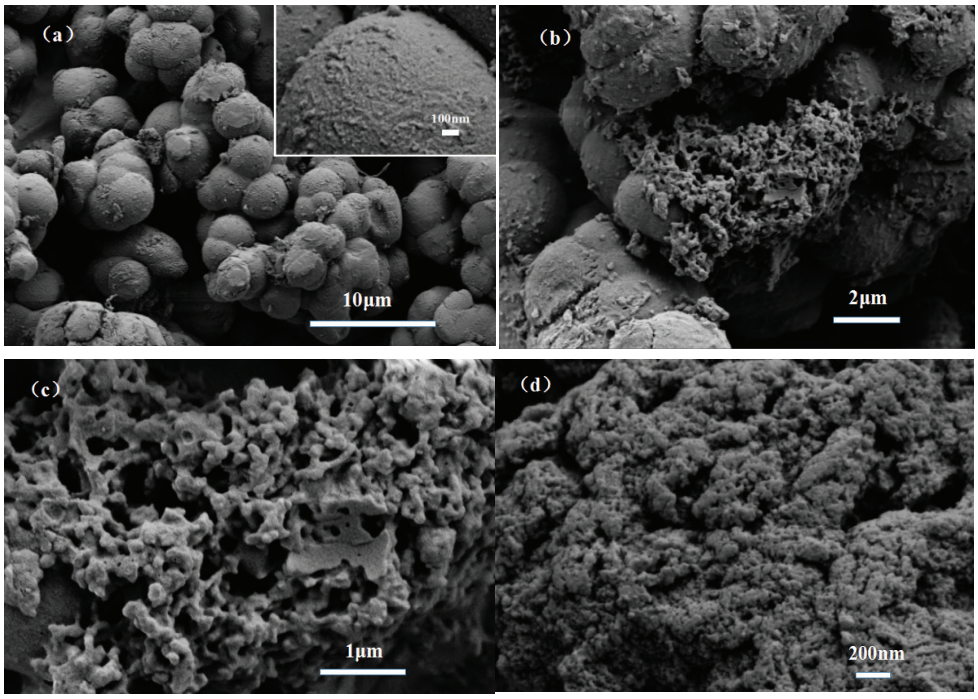

Fig. 5. SEM images of PIM-1 (a–c) and NH_2-PIM-1 (d).

lapsed and squeezed. This was consistent with N_2 adsorption isotherms. Compared to PIM-1, although the surface area of NH_2-PIM-1 was slightly decreased, the active sites increased due to the introduction of amine groups. Therefore, NH_2-PIM-1 could be used as an efficient adsorbent.

3.1.3. TGA

Thermal analysis experiments of PIM-1 and NH_2-PIM-1 were employed and the results were shown in Fig. 6. There was total weight loss of 31.2%for PIM-1 at 425–600°C which attributed to the decomposition of the skeletal structure. While two weight-loss stages of NH_2-PIM-1 were observed as the temperature was increased from 50°C to 800°C. The first one was from 350 to 425°C with a total weight loss of 5.2% which attributed to the degradation of the amine groups and residual solvent. The second weight loss (425–600°C) with a total weight loss of 30.1% could be ascribed to the decomposition of the skeletal structure which was similar to PIM-1.

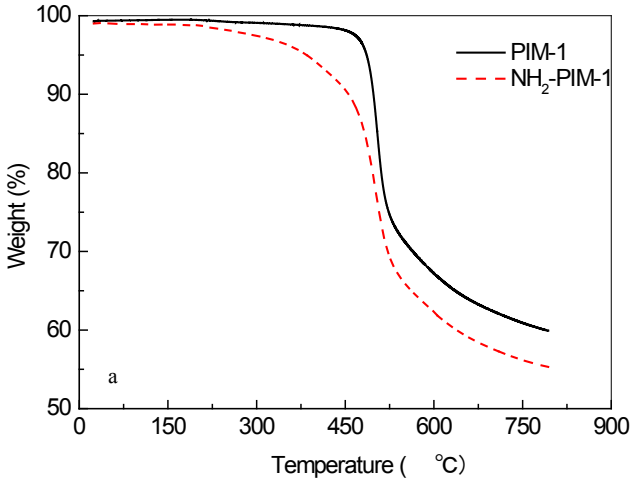

Fig. 6 Thermogravimetric analysis of PIM-1 and NH_2-PIM-1.

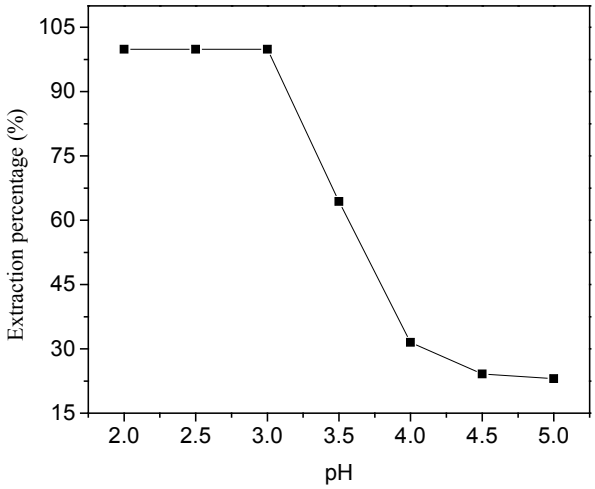

Fig. 7. Effect of pH on the extraction percentage. Condition: sample volume: 10 mL; initial concentration: 100 mg/L; amount of adsorbent: 5 mg; contact time: 1 h; temperature: 298 K.

3.3. Betch experiments

3.3.1. Effect of pH

The initial pH of the dye solutions was an important factor to controls the adsorption process, because it can change the charge of the adsorbents' surface and ionization of dyes [24]. The effects of initial solution pH on SY adsorption onto NH_2-PIM-1 was studied by varying the pH value from 2.0 to 5.0 at room temperature. With increasing the acidity of the solution, the functional group (–NH_2) of NH_2-PIM-1 could change into ammonium cation(–NH_3^+). As shown in Fig. 7, percentage adsorption of SY increased gradually with decreasing pH from 5.0 to 2.0. As the pH value decreased from 5.0 to 3.0, the trend was that the extraction percentage of SY significantly increased from 23.05% to 99.90%. The protonation degree of –NH_2 on the surface of the adsorbents increased with decreasing pH value, thereby further increase of SY adsorption might be due to the electrostatic attraction on the positively charged sites of NH_2-PIM-1 [34]. However, with the solution pH value reducing below 3.0, the extraction percentage was still 99.90%. The reason may be attributed to the amine (–NH_2) on NH_2-PIM-1 could be completely protonated to cationic group, and the electrostatic attractions between the adsorbent and adsorbate would keep constant. Thus pH 2.5 was selected as the pH condition for the following studies.

3.3.2. Effect of adsorbent dosage

To investigate the effect of the amount of NH_2-PIM-1 on the extraction percentage for SY, 10 mL solution containing 100 mg/L of SY at pH 2.5 was stirred for 1 h with different amount of NH_2-PIM-1 ranging from 1.0 to 9.0 mg. The results indicated that the adsorption effect for SY increased significantly by increasing the dosage of adsorbent from 1.0 to 9.0 mg, with 5.0 mg as the inflection point. From 1.0 to 5.0 mg, the promotion of the extraction percentage was significantly while the increase of extraction was not obvious after 5.0 mg. Therefore, 5.0 mg was the optimal amount of adsorbent.

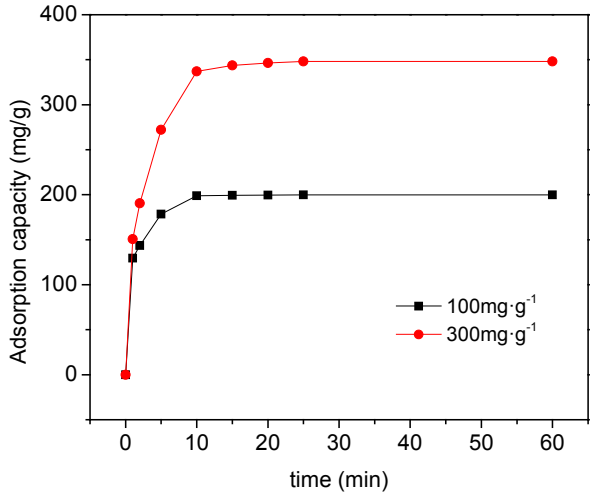

Fig. 8. Effect of contact time on the adsorption capacity. Condition: solution pH: 2.5; amount of adsorbent: 5 mg; other conditions can be seen in Fig. 7.

3.3.3. Effect of contact time

The effect of the contact time on the adsorption of SY was investigated at room temperature, with initial concentration of 100 and 300 mg/L respectively (as shown in Fig. 8). For both concentrations, the extraction percentage increased with high slope during the initial stage. But after inflection point, the growth rates become lower. The equilibrium was achieved after 10 min, which was faster than most of the previous works (shown in Table 1). The possible explanation for the observed curve could be that most vacant surface sites are available for adsorption at the initial stage, while the SY molecules were difficult to load on the remaining vacant surface sites with the increasing of contact time due to the increasing repulsive forces between the SY molecules and NH_2-PIM-1. In this experiment, the adsorption equilibrium time was selected for the contact time of 10 min.

Table 1
Comparison of SY adsorption performance of various adsorbents

Adsorbents	Contact time (min)	Adsorption capacity (mg/g)	Ref.
$Cd(OH)_2$-NW-AC	15–30	80.6	[3]
MWCNT-PATMSPEDA-Pd-NPs	4	59.7	[18]
Ce/C_{KIT-6}	70	223.91–323.91	[19]
CaAl-LDH-NO_3	50	398.41	[26]
$Zn(OH)_2$-NP-AC	5.2	115	[35]
PMO-IL	2	192.3–208.3	[36]
PDVB-IL	300	734.62	[37]
ZnO-NPs-AC	10	142.85	[38]
CdTN-AC	28	61.31	[39]
NH_2-PIM-1	10	348.16	This study

3.3.4. Effect of initial SY concentration

The initial concentration of SY was an important factor to affect the capacity of adsorption. To further investigate the maximum adsorption capacity of NH_2-PIM-1, the experiments with SY concentrations ranging from 100 to 500 mg/L were designed at three temperatures (283, 298 and 313K), respectively. As shown in Fig. 9, the adsorption equilibria were obtained after 200 mg/L for different temperatures. The maximum adsorption capacities were 304.38, 348.16 and 372.43 mg/g, respectively, corresponding to 283, 298 and 313K, which indicates that higher adsorption capacity can be obtained at higher temperature. It was found that the maximum adsorption capacity at room temperature of NH_2-PIM-1 was higher than most of the previous reported adsorbents (shown in Table 1), which could be attributed to (the high surface area and functional groups) the addition of amino groups. Thus, NH_2-PIM-1 could be applied as a very efficient adsorbent of sunset yellow FCF with high adsorption capacity and low time cost.

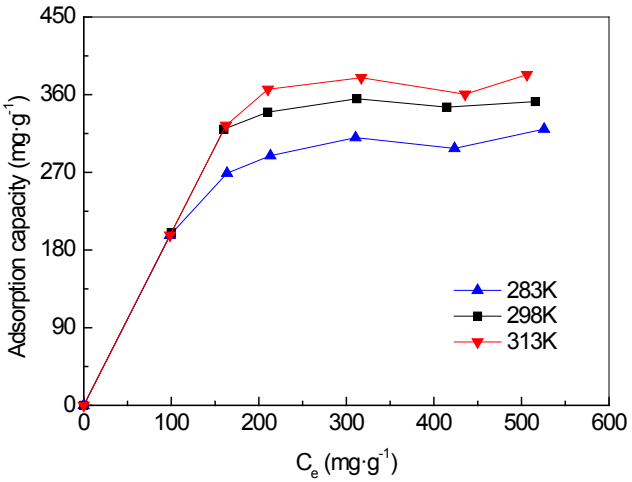

Fig. 9. Effect of initial concentration on adsorption capacity. Condition: solution pH: 2.5; amount of adsorbent: 5 mg; contact time: 10 min; other conditions can be seen in Fig. 7.

3.4. Adsorption kinetics

Adsorption kinetics were studied by fitting the experimental data with the pseudo-first-order kinetic model and pseudo-second-order kinetic model [40], respectively. The model equations are as follows:

$$\ln(Q_e - Q_t) = \ln Q_e - k_1 t \quad (3)$$

$$t / Q_t = t / Q_e + 1 / (k_2 Q_e^2) \quad (4)$$

In Eqs. (3) and (4), Q_e and Q_t are the amounts of adsorbed SY at equilibrium and at time t (min), respectively, k_1 and k_2 are the equilibrium rate constant of pseudo-first-order sorption (min^{-1}) and pseudo-second-order sorption ($g \cdot mg^{-1} \cdot min^{-1}$), respectively.

The plots of the linearized form of these models for the adsorption were showed in Fig. 10. As depicted in Table 2, in the calculation of pseudo-second order equation and pseudo-first-order equation, inaccurate sampling and inaccurate testing within the error range may result in the difference between Q_{cal} value and Q_{exp} value [41]. However, the pseudo-second-order equation was more consistent with the experimental kinetic data than pseudo-first-order equation because of the larger value of linear regression coefficients (R^2) in treating 100 mg/L and 300 mg/L of the SY concentration, which indicated the adsorption process of SY by NH_2-PIM-1 from aqueous solution can be well described by the pseudo-second-order model.

3.5. Adsorption isotherms

The adsorption isotherm model revealed the mechanism of interaction between adsorbates and adsorbents [40]. Langmuir and Freundlich isotherm models [42] were studied to analyze the equilibrium adsorption data. The models could be described by the following equations, respectively.

$$C_{eq} / Q_{eq} = C_{eq} / Q_{\max} + 1 / (bQ_{\max}) \quad (5)$$

$$\lg Q_{eq} = (1/n) \lg C_{eq} + \lg K \quad (6)$$

In Eqs. (5) and (6), Q_{eq} is the amount of adsorbed SY in the adsorbent (mg/g), C_{eq} is the equilibrium concentration in solution (mg/L), Q_{eq} is the maximum adsorption capacity (mg/g), b is the Langmuir constant (L/mg), K and n are the Freundlich constants. The adsorption isotherms were simulated by the Langmuir and Freundlich isotherm models (Fig. 11), and Table 3 showed the parameters of the Langmuir and Freundlich isotherms. The Langmuir adsorption model had a higher R^2 value and the adsorption capacity was calculated by Langmuir adsorption model conform to the experimental value, indicating the adsorption isotherm can be depicted by the Langmuir isotherm model at three temperatures and the active sites on NH_2-PIM-1 were homogeneous.

3.6. Thermodynamic studies

The thermodynamic parameters such as standard free energy change ΔG^o (kJ/mol), standard entropy change ΔS^o

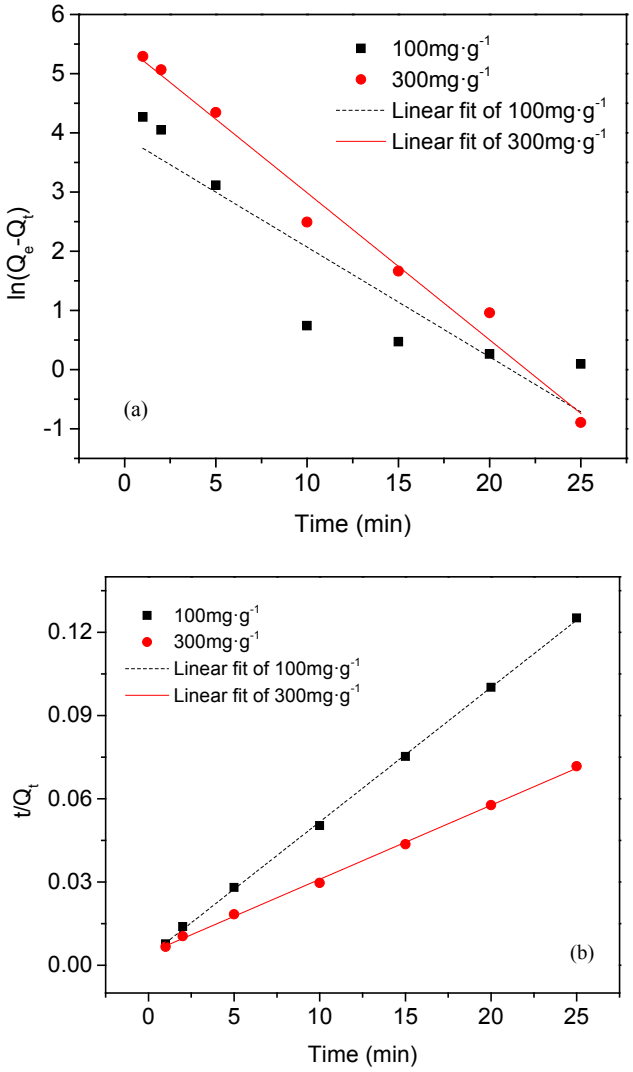

Fig. 10. Adsorption kinetics of SY on NH_2-PIM-1. (a) pseudo-first order; (b) pseudo-second order models.

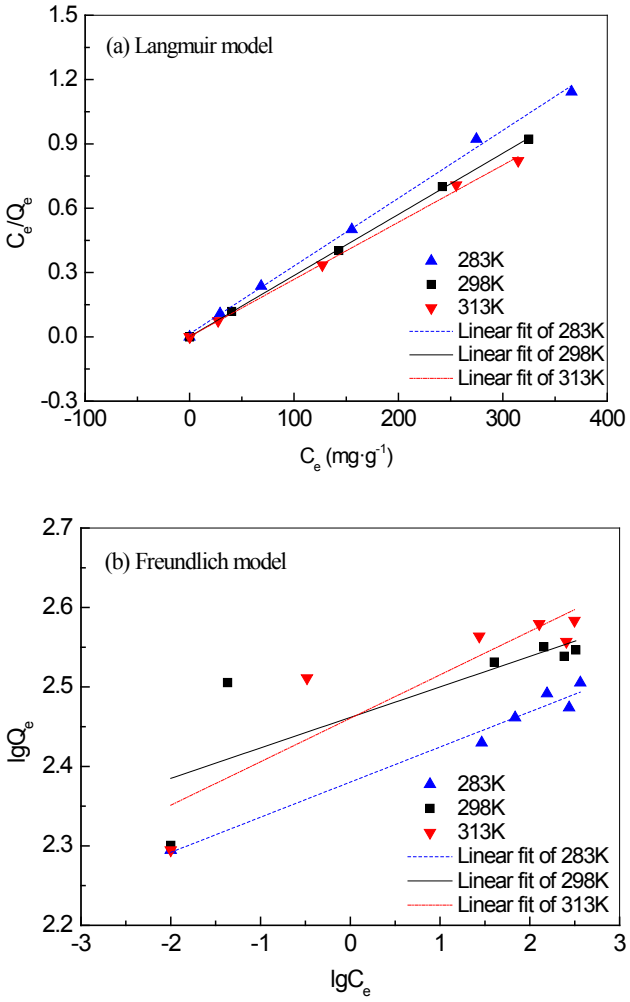

Fig. 11. Adsorption isotherm of SY on NH_2-PIM-1. (a) Langmuir and (b) Freundlich models.

Table 2
Adsorption kinetic parameters of SY on NH_2-PIM-1

Concentration (mg/L)	Q_{exp} (mg/g)	Pseudo-first-order model			Pseudo-second-order model		
		R^2	Q_{cal} (mg/g)	k_1 (min^{-1})	R^2	Q_{cal} (mg/g)	$k_2 \times 10^2$ (g/(mg·min))
100	199.80	0.8378	50.65	0.1856	0.9996	208.33	0.72
300	348.16	0.9841	238.05	0.2485	0.9989	370.38	0.17

Table 3
Langmuir and Freundlich isotherms

Temperature (K)	Q_{exp} (mg/g)	Langmuir parameters			Freundlich parameters		
		Q_{cal} (mg/g)	b (L/mg)	R^2	n	K	R^2
283	304.38	316.06	0.227	0.9975	22.63	240.05	0.9735
298	348.16	350.63	3.768	0.9998	26.06	289.53	0.6413
313	372.43	375.09	2.216	0.9984	18.28	288.80	0.8186

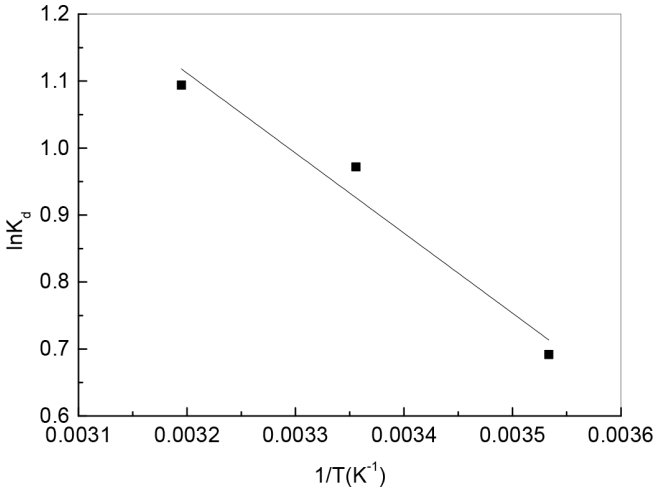

Fig. 12. Plot of ln K_d vs 1/T for adsorption of SY onto NH_2-PIM-1.

($J \cdot mol^{-1} \cdot K^{-1}$) and standard enthalpy change ΔH^o (kJ/mol), were calculated using the following equations [43].

$$K_d = (C_0 - C_e)V / (C_e W) \quad (7)$$

$$\Delta G^0 = -RT \ln K_d \quad (8)$$

$$\ln K_d = \Delta S^0 / R - \Delta H^0 / (RT) \quad (9)$$

In Eqs. (7), (8) and (9), K_d is distribution adsorption coefficient, R is the gas constant (8.314×10^{-3} $J \cdot mol^{-1} \cdot K^{-1}$) and T is the Kelvin temperature (K). The values of ΔH^o and ΔS^o are determined from the slope and intercept of van't Hoff plots of ln K_d vs. 1/T, respectively (Fig. 12). Table 4 showed the thermodynamic parameters of NH_2-PIM-1, and the coefficient of determination R^2 reached to 0.9256. Ozcan et al. [44] claimed that the adsorption was physisorption if ΔG^o was in range of –20 to 0 kJ/mol. Otherwise, the adsorption was chemisorption if the range was between –80 and –400 kJ/mol. In our study, the ΔG^o values were in range of –1.592 to –2.785 kJ/mol, which showed that physical adsorption played a dominant role in SY adsorption on NH_2-PIM-1. Also, the ΔH^o value was positive (9.933 kJ/mol), suggesting the process was an endothermic physisorption [45]. The positive values of ΔS^o respectively expressed an increased randomness at the interface between solid and solution. Moreover, the value of ΔG^o was more negative as the temperature increased, indicating a high temperature facilitates the spontaneity of the adsorption of SY on NH_2-PIM-1.

Table 4
Thermodynamic parameters for SY adsorption on NH_2-PIM-1

Dye	ΔH^o ($kJ \cdot mol^{-1}$)	ΔS^o ($J \cdot mol^{-1} \cdot K^{-1}$)	ΔG^o ($kJ \cdot mol^{-1}$)		
			283K	298K	313K
Sunset Yellow FCF	9.933	41.03	–1.592	–2.356	–2.785

4. Conclusions

In this work, an efficient adsorbent (NH_2-PIM-1) with a high specific surface area (593.03 $m^2 \cdot g^{-1}$) was successfully synthesized by reducing nitriles to amines in the polymer of intrinsic microporosity (PIM-1), which was applied to remove anionic dye sunset yellow FCF (SY) from aqueous solutions. The physicochemical properties of NH_2-PIM-1 were characterized by different techniques such as SEM, BET, TGA and FTIR. The adsorption process could be better modeled by Langmuir isotherm equation and pseudo-second-order kinetic equation, providing $R^2 > 0.997$.The adsorption capacity of SY on NH_2-PIM-1 could reach 348.16 mg/g within 10 min, which was probably contributed by the porous structure and the amine modification. Owing to the high surface areas, low-cost and high efficiency, NH_2-PIM-1 had great potential application as efficient adsorbent to solve environmental pollution in possible real work.

Acknowledgements

This work was supported by National Natural Science Foundation (21307013, 21377024, and 21375019), Program for New Century Excellent Talents in Fujian Province University (JA14027) and Natural Science Foundation of Fujian Province (2015J01044).

Conflicts of Interest

The authors declare no conflict of interest.

References

[1] M. Ghaedi, N. Mosallanejad, Study of competitive adsorption of malachite green and sunset yellow dyes on cadmium hydroxide nanowires loaded on activated carbon, J. Ind. Eng. Chem., 20 (2014) 1085-1096.
[2] J.S. Piccin, L.A. Feris, M. Cooper, M. Gutterres, Dye adsorption by leather waste: mechanism diffusion, nature studies, and thermodynamic data, J. Chem. Eng. Data, 58 (2013) 873–882.

[3] P. Semeraro, V. Rizzi, P. Fini, Interaction between industrial textile dyes and cyclodextrins, Dyes Pigm., 119 (2015) 84–94.
[4] D. Shen, J. Fan, W. Zhou, B. Gao, Q. Yue, Q. Kang, Adsorption kinetics and isotherm of anionic dyes onto organo-bentonite from single and multisolute systems, J. Hazard. Mater., 172 (2009) 99–107.
[5] Z. Yang, H. Yang, Z. Jiang, T. Cai, H. Li, H. Li, A. Li, R. Cheng, Flocculation of both anionic and cationic dyes in aqueous solutions by the amphoteric grafting flocculant carboxymethyl chitosan-graft-polyacrylamide, J. Hazard. Mater., 254–255 (2013) 36–45.
[6] F.C. Moreira, S. Garcia-Segura, V.J. Vilar, R.A. Boaventura, E. Brillas, Decolorization and mineralization of Sunset Yellow FCF azo dye by anodic oxidation, electro-Fenton, UVA photoelectro-Fenton and solar photoelectro-Fenton processes, Appl. Catal., 142 (2013) 877–890.
[7] Z. Jing, C. Shuo, Z. Ying, Q. Xie, Z. Huimin, Z. Yaobin, Reduction of acute toxicity and genotoxicity of dye effluent using Fenton-coagulation process, J. Hazard. Mater., 274 (2014) 198–204.
[8] I. Khouni, B. Marrot, P. Moulin, R.B. Amar, Decolourization of the reconstituted textile effluent by different process treatments: enzymatic catalysis, coagulation/flocculation and nanofiltration processes, Desalination, 268 (2011) 27–37.
[9] V. Kuzhalosai, B. Subash, A. Senthilraja, P. Dhatshanamurthi, M. Shanthi, Synthesis, characterization and photocatalytic properties of SnO_2-ZnO composite under UV-A light, Spectrochim. Acta. Part A, 115 (2013) 876–882.
[10] S. Kalleary, F.M. Abbas, A, Ganesan, S. Meenatchisundaram, B. Srinivasan, A.S.B. Packirisamy, R.k. Kesavan, S. Muthusamy, Biodegradation and bioelectricity generation by microbial desalination cell, Int. Biodeterior. Biodegrad., 92 (2014) 20–25.
[11] Y. Wanga, J. Zhua, G. Donga, Y. Zhang, N. Guoa, J. Liua, Sulfonated halloysite nanotubes/polyethersulfone nanocomposite membrane for efficient dye purification, Sep. Purif. Technol., 150 (2015) 243–251.
[12] J. Zhao, Q. Huang, M. Liu, et al. Synthesis of functionalized MgAl-layered double hydroxides via modified mussel inspired chemistry and their application in organic dye adsorption, J. Colloid. Inter. Sci., 505 (2017) 168–177.
[13] N. Kumar, L. Reddy, V. Parashar, J.C. Ngila, Controlled synthesis of microsheets of ZnAl layered double hydroxides hexagonal nanoplates for efficient removal of Cr(VI) ions and anionic dye from water, J. Environ. Chem. Eng., 5 (2017) 1718–1731.
[14] K.B. Tana, M. Vakilib, B.A. Horria, P.E. Poha, A.Z. Abdullahc, B. Salamatiniaa, Adsorption of dyes by nanomaterials: recent developments and adsorption mechanisms, Sep. Purif. Technol., 150 (2015) 229–242.
[15] S.M.A. Mohd, M.D. Khalid, K.W.A.W. Abdul, I. Azni, Cationic and anionic dye adsorption by agricultural solid wastes: A comprehensive review, Desalination, 280 (2011) 1–13.
[16] T. Wua, Q. Shao, S. Gea, L. Bao, Q. Liua, The facile preparation of novel magnetic zirconia composites with the aid of carboxymethyl chitosan and their efficient removal of dye, RSC Adv., 6 (2016) 58020–58027.
[17] Y. Liu, J. Li, Y. Yang, B. Li, Facile immobilization of polyaspartate onto silica gels via poly (dopamine) for the removal of methylene blue from aqueous solution, Appl. Surf. Sci., 315 (2015) 831–839.
[18] R. Karimi, F. Yousefi, M. Ghaedi, K. Dashtian, M. Montazerozohori, Efficient adsorption of erythrosine and sunset yellow onto modified palladium nanoparticles with a 2-diamine compound: Application of multivariate technique, J. Ind. Eng. Chem., 48 (2017) 43–55.
[19] L.T. Horng, Development of mesoporous structure and high adsorption capacity of biomass-based activated carbon by phosphoric acid and zinc chloride activation, Chem. Eng. J., 158 (2010) 129–142.
[20] S. Kim, Y.M. Lee, Rigid and microporous polymers for gas separation membranes, Prog. Polym. Sci., 43 (2015) 1–32.
[21] M.U. Dura, L. Cavas, S.K. Papageorgiou, F.K. Katsaros, Methylene blue adsorption on activated carbon prepared from Posidonia oceanica (L.) dead leaves: Kinetics and equilibrium studies, Chem. Eng. J., 168 (2011) 77–85.
[22] S. Xiao, M. Shen, R. Guo, Q. Huang, S. Wang, X. Shi, Fabrication of multiwalled carbon nanotube-reinforced electrospun polymer nanofibers containing zero-valent iron nanoparticles for environmental applications, J. Mater. Chem., 20 (2010) 5700–5708.
[23] D. Wesenberg, I. Kyriakides, S.N. Agathos, White-rot fungi and their enzymes for the treatment of industrial dye effluents, Biotechnol. Adv., 22 (2003) 161–187.
[24] B. Satilmis, T. Uyar, Removal of aniline from air and water by polymers of intrinsic microporosity (PIM-1) electrospun ultrafine fibers, J. Colloid Interf. Sci., 516 (2018) 317–324.
[25] B. Satilmis, M.N. Alnajrani, P.M. Budd, Hydroxyalkylaminoalkylamide PIMs: selective adsorption by ethanolamine-and diethanolamine-modified PIM-1, Macromol., 48 (2015) 5663–5669.
[26] P. de Sá, B.N. Cunha, L.M. Nunes, Effect of pH on the adsorption of Sunset Yellow FCF food dye into a layered double hydroxide (CaAl-LDH-NO_3), Chem. Eng. J., 215 (2013) 122–127.
[27] B. Satilmis, P.M. Budd, Base-catalysed hydrolysis of PIM-1: amide versus carboxylate formation, RSC Adv., 4 (2014) 52189–52198.
[28] C. Zhang, P. Li, B. Cao, Electrospun polymer of intrinsic microporosity fibers and their use in the adsorption of contaminants from a nonaqueous system, J. Appl. Polym. Sci., 133 (2016) 1–10.
[29] C.S. Chiou, J.S. Shih, Bifunctional cryptand modifier for capillary electrophoresis in separations of inorganic/organic anions and inorganic cations, Anal., 121 (1996) 1107–1110.
[30] Y.F. Lin, H.W. Chen, P.S. Chien, C.S. Chiou, C.C. Liu, Application of bifunctional magnetic adsorbent to adsorb metal cations and anionic dyes in aqueous solution, J. Hazard. Mater., 185 (2011) 1124–1130.
[31] C.C. Liu, M. Kuang-Wang, Y.S. Li, Removal of nickel from aqueous solution using wine processing waste sludge, Ind. Eng. Chem. Res., 44 (2005) 1438–1445.
[32] N. Li, R. Bai, C. Liu, Enhanced and selective adsorption of mercury ions on chitosan beads grafted with polyacrylamide via surface-initiated atom transfer radical polymerization, Langmuir, 21 (2005) 11780–11787.
[33] C.R. Mason, L. Maynard-Atem, K.W. Heard, B. Satilmis, P.M. Budd, K. Friess, M. Lanc, P. Bernardo, G. Clarizia, J.C. Jansen, Enhancement of CO_2 affinity in a polymer of intrinsic microporosity by amine modification, Macromolecules, 47 (2014) 1021–1029.
[34] M. Min, L. Shen, G. Hong, et al. Micro-nano structure poly(ether sulfones)/poly(ethyleneimine) nanofibrous affinity membranes for adsorption of anionic dyes and heavy metal ions in aqueous solution, Chem. Eng. J., 197(14) (2012) 88–100.
[35] M. Roostaa, M. Ghaedia, R. Sahraeib, M.K. Purkaitc, Ultrasonic assisted removal of sunset yellow from aqueous solution by zinc hydroxide nanoparticle loaded activated carbon: Optimized experimental design, Mater. Sci. Eng.: C, 52 (2015) 82–89.
[36] M. Ghaedi, D. Elhamifar, M. Roosta, R. Moshkelgosha, Ionic liquid based periodic mesoporous organosilica: an efficient support for removal of sunset yellow from aqueous solutions under ultrasonic conditions, J. Ind. Eng. Chem., 20 (2014) 1703–1712.
[37] H. Gao, T. Kan, S. Zhao, Y. Qian, X. Cheng, W. Wu, X. Wang, L. Zheng, Removal of anionic azo dyes from aqueous solution by functional ionic liquid cross-linked polymer, J. Hazard. Mater., 261 (2013) 83–90.
[38] M. M, G. M, Z. A, G. AM, H. MH, Artificial neural network (ANN) method for modeling of sunset yellow dye adsorption using zinc oxide nanorods loaded on activated carbon: Kinetic and isotherm study, Spectrochim. Acta Part A: Molec. Biomolec. Spectroscopy, 134 (2015) 1–9.
[39] M. Ghaedi, A. Hekmati Jah, S. Khodadoust, R. Sahraei, A. Daneshfar, A. Mihandoost, M.K. Purkait, Cadmium telluride nanoparticles loaded on activated carbon as adsorbent for removal of sunset yellow, Spectrochim. Acta Part A: Molec. Biomolec. Spectroscopy, 90 (2012) 22–27.

[40] W. Xinpeng, L. Zhiming, Y. Xiangping, H. Kun, Z. Huiqing, Y. Jianfeng, J. Mei, G. Zhouyi, A facile one-step approach to functionalized graphene oxide-based hydrogels used as effective adsorbents toward anionic dyes, Appl. Super. SCI., 308 (2014) 82–90.
[41] P. BN, M. D, Removal of anionic dyes from water by potash alum doped polyaniline: investigation of kinetics and thermodynamic parameters of adsorption, J. Phys. Chem. B, 119 (2015) 8154–8164.
[42] L. Yu, Y. Luo, The adsorption mechanism of anionic and cationic dyes by Jerusalem artichoke stalk-based mesoporous activated carbon, J. Environ. Chem. Eng., 2 (2014) 220–229.
[43] N.B.H. Abdelkader, A. Bentouami, Z. Derriche, N. Bettahar, L.C. de Ménorval, Synthesis and characterization of Mg–Fe layer double hydroxides and its application on adsorption of Orange G from aqueous solution, Chem. Eng. J., 169 (2011) 231–238.
[44] A. Ozcan, E.M. Oncu, S. Ozcan, Kinetics, isotherm and thermodynamic studies of adsorption of acid blue 193 from aqueous solutions onto natural sepiolite, Colloids Surf. A: Physicochem. Eng. Aspects, 277 (2006) 90–97.
[45] C.Y. Kuo, C.H. Wu, J.Y. Wu, Adsorption of direct dyes from aqueous solutions by carbon nanotubes: determination of equilibrium, kinetics and thermodynamics parameters, J. Colloid. Inter. Sci., 327 (2008) 308–315.